The LINNEAN SOCIETY of London BOTANICAL Journal of the Linnean Society

Botanical Journal of the Linnean Society, 2016, **182**, 256–271. With 4 figures

Phylogenetics and diversification history of African rattans (Calamoideae, Ancistrophyllinae)

ADAMA FAYE[1], JEAN-CHRISTOPHE PINTAUD[1], WILLIAM J. BAKER FLS[4], YVES VIGOUROUX[1], BONAVENTURE SONKE[2] and THOMAS L. P. COUVREUR[1,2,3]*

[1]*Institut de Recherche pour le Développement, UMR-DIADE, BP 64501, F-34394 Montpellier Cedex 5, France*
[2]*Département des Sciences Biologiques, Laboratoire de Botanique systématique et d'Ecologie, Université de Yaoundé I, Ecole Normale Supérieure, BP 047 Yaoundé, Cameroon*
[3]*Botany Section, Naturalis Biodiversity Centre, Darwinweg 2, 2333 CR Leiden, the Netherlands*
[4]*Royal Botanic Gardens, Kew, Richmond, Surrey, TW9 3AB, UK*

Received 9 December 2015; revised 28 April 2016; accepted for publication 31 May 2016

Even though African rain forests display high levels of local species diversity and endemism, their lower continental species diversity when compared with the Neotropics and Asia is paradoxical. This disparity is mainly thought to be linked to either important extinction events during the Pleistocene or at the Eocene–Oligocene boundary. African rattans or climbing palms are one of the most diverse clades of palms in Africa, representing one-third of all known species. Here, we reconstruct the phylogeny and temporal evolution of African rattans (Arecaceae: Calamoideae: Lepidocaryeae: Ancistrophyllinae) to test the two main hypotheses of palm evolution in Africa. We constructed a near-complete, dated species-level phylogenetic tree for subtribe Ancistrophyllinae using plastid and nuclear markers. The generic relationships between Ancistrophyllinae were fully resolved and species-level relationships are well to weakly supported. Ancistrophyllinae diversified during the Eocene with most species originating during the late Miocene after 10 Mya. This result is in agreement with several other studies suggesting a pre–Pleistocene origin of the extant African flora. Ancistrophyllinae display an anti-sigmoidal lineage-through-time plot with a moderate overall extinction fraction. Our simulations suggest important roles for an ancient extinction event at the Oligocene–Eocene boundary. In contrast, the hypothesis of an important extinction event in palms during the late Pliocene at 3 Mya is not supported. We suggest that the evolutionary history of African rattans has undergone a constant diversification rate punctuated by one or several important extinction events during the first part of the Cenozoic with most species diversity accumulating during the late Miocene and Pliocene. © 2016 The Linnean Society of London, *Botanical Journal of the Linnean Society*, 2016, **182**, 256–271

ADDITIONAL KEYWORDS: LTT plots – molecular dating – palms – phylogenetic – simulations.

INTRODUCTION

With 21 currently recognized species, the endemic African rattan genera (Calamoideae: Lepidocaryeae: Ancistrophyllinae) account for one-third of all African palm species diversity (Stauffer, Ouattara & Stork, 2014). *Eremospatha* (G.Mann & H.Wendl.) Schaedtler (11 species), *Laccosperma* (G. Mann & H. Wendl.) Drude (six species) and *Oncocalamus* (G. Mann & H. Wendl.) H.Wendl. (four species) are mainly distributed in Central and West African lowland rain forests (Sunderland, 2012). Morphological and molecular studies have clearly shown that these three genera form a monophyletic group (Baker, Dransfield & Hedderson, 2000a; Baker, Hedderson & Dransfield, 2000b; Asmussen *et al.*, 2006; Baker *et al.*, 2009; Faye *et al.*, 2014) and they all share a set of unique morphological characters (Baker *et al.*, 2000a) such as the presence of a whip-like extension of the rachis (called a cirrus), generally bearing numerous modified hook-like leaflets termed acanthophylls, and inflorescences that are not adnate to

*Corresponding author. E-mail: thomas.couvreur@ird.fr

either the stem internode or leaf sheath. Beside these common characters, each genus is easily distinguished by morphological and reproductive characters, such as the presence or absence of spines on the leaf sheaths, spines being flat or rounded and hapaxanthic versus pleonanthic reproductive systems (Sunderland, 2012; Faye *et al.*, 2014). Despite these differences their phylogenetic relationships at generic and species levels remain poorly understood (Baker *et al.*, 2000a,b, 2009; Asmussen *et al.*, 2006; Faye *et al.*, 2014). In the most comprehensive study to date based on four plastid markers with 80% of species sampled (Faye *et al.*, 2014), the relationships between the genera could not be resolved.

Even though some African rain forests contain high levels of alpha diversity and endemism at local levels (e.g. Gentry, 1993; Kenfack *et al.*, 2007) tropical Africa has been labelled as the 'odd man out' in terms of continental species diversity (Richards, 1973). Numerous hypotheses have been suggested to explain this pattern of lower species diversity in Africa (reviewed by Couvreur, 2015) ranging from the impact of current and past climate, alternative diversification/extinction rates between regions, alternative human impacts or more recently the role of the African megafauna such as elephants (Terborgh *et al.*, 2016) or the extension of C4 savannas across Africa (Linder, 2014). Palms are a characteristic tropical rain forest plant family and have been proposed as a model group for studying the evolution of tropical rain forests (Couvreur & Baker, 2013). They provide an ideal example of species richness discrepancies between the major continental rain forest blocks (Dransfield, 1988) reflecting the 'odd man out pattern'. There are ~1200 species of palms in tropical Asia (India to the Solomon Islands), 730 in the Americas, ~200 in Madagascar and only 65 in Africa (Dransfield *et al.*, 2008; Rakotoarinivo *et al.*, 2014). Because regional species diversity is mainly the result of historical events linked to speciation and extinction rates (Ricklefs, 2005), one of the main hypotheses advanced to explain this lower species diversity is that the African flora underwent higher extinction rates when compared with other regions during the Cenozoic (Axelrod & Raven, 1978; Richards, 1996; Morley, 2000; Couvreur, 2015). This explanation has also been advanced by several authors for the African palms, but at contrasting periods (Moore, 1973; Dransfield, 1988; Baker & Dransfield, 2000; Pan *et al.*, 2005; Blach-Overgaard *et al.*, 2010, 2013, 2015; Kissling *et al.*, 2012a). For palms, two major periods during the Cenozoic have been suggested as important in explaining present day lower diversity across Africa: 1. Ancient extinction event: the Eocene–Oligocene boundary at 33 Mya represents a drastic and sudden decline in global temperatures (Zachos *et al.*, 2001) and is generally referred to as the 'big chill' (Morley, 2000). This event is thought to be responsible for the extinction of numerous plant groups and palms in particular (Salard-Cheboldaeff, 1990; Morley, 2000). The analyses of the fossil flora of Chilga in Ethiopia showed that the Eocene–Oligocene boundary was possibly responsible for a major decrease in the number of African palm morphospecies (Pan *et al.*, 2005) and was suggested as an important reason for explaining the lower diversity of palms in Africa. 2. Recent extinction event: the late Pliocene/early Pleistocene (3.5–1.6 Mya) was a period of pronounced drying and cooling phases in Africa, the most important one occurring around 3 Mya (Morley, 2000). The fossil record documents widespread grass-dominated ecosystems at that time (Jacobs, Kingston & Jacobs, 1999). This increased continental aridity was partly the result of major uplifts of several parts of the East African Rift System during the late Pliocene leading to a change in atmospheric circulation (Sepulchre *et al.*, 2006). Numerous extinction events are documented in the fossil record at that time, including some for palms (Morley, 2000). Moore (1973) suggested that these climatic events were the main reason for the lower African palm diversity. Kissling *et al.* (2012b), based on a global analysis of palm phylogenetic structure, found a random phylogenetic structure for African palms and suggested that this was the result of important Quaternary climatic oscillations preventing the diversification of rain forest lineages in palms.

Even though estimating extinction and speciation rates from molecular phylogenetic trees is challenging (Rabosky, 2010; Morlon, 2014; Beaulieu & O'Meara, 2015), understanding how species have diversified through time can provide important insights into how the African palm flora has assembled (Linder, 2001). To date no species-level, dated phylogenetic tree for African palms has been published, hampering our understanding of the origin of palm diversity in Africa. The family-wide, dated phylogenetic tree for palms (Baker & Couvreur, 2013a) estimated that Ancistrophyllinae originated at the end of the Cretaceous period (70 Mya, stem node), with the three genera originating during the Eocene period (47–31 Mya). Thus the evolutionary history of this clade spans a long period ideal to test the above hypotheses. The present paper aims: (1) to clarify the phylogenetic relations in Ancistrophyllinae based on a broad sampling of taxa and molecular markers; and (2) to test if present day species diversity in Ancistrophyllinae is the result of ancient or more recent extinction events.

MATERIAL AND METHODS

Species data

This study combined published plastid sequence data (Faye *et al.*, 2014) with newly sequenced plastid and nuclear sequence data. Sequence data for both plastid and nuclear markers were produced for 28 individuals representing 18 species (Table 1) (out of the currently recognized 21 species) (Sunderland, 2012). *Laccosperma laeve* (G. Mann & H. Wendl.) Kuntze is newly sequenced here. For three species [*L. secundiflorum* (P.Beauv.) Kuntze, *L. opacum* Drude and *L. robustum* (Burret) J.Dransf.], two individuals were sequenced from different geographical regions because these species are widespread and are morphologically variable. Six outgroup species belonging to different subtribes of Calamoideae following Faye *et al.* (2014) were also included.

DNA extraction, amplification and sequencing

Total genomic DNA was extracted following the same protocol as in Faye *et al.* (2014). Plastid DNA markers [*psbA–trnH* (Al-Qurainy *et al.*, 2011), *psbZ–trnFM*, *atpI–atpH* and *rps3–rpl16* (Scarcelli *et al.*, 2011)] were sequenced for the additional taxa included in this study using Sanger sequencing following Faye *et al.* (2014). To sequence as many nuclear markers as possible we followed the targeted amplicon sequencing (TAS) approach (Bybee *et al.*, 2011). We targeted five common nuclear markers used in palm phylogenetics: PRK (Lewis & Doyle, 2002), RPB2 (Roncal *et al.*, 2005), WRKY7 (Mauro-Herrera *et al.*, 2006; Meerow *et al.*, 2009), malate synthase (Lewis & Doyle, 2001) and AGAMOUS 1 (Ludeña *et al.*, 2011). All nuclear and plastid markers used for PCR are available in the Table 2. The TAS approach (see Data S1) combined two PCR steps before sequencing (Bybee *et al.*, 2011). Samples for this study were sent to MWG for sequencing using the 454 GS FLX+ chemistry. In total 145 sequences were newly generated in this study (all nuclear markers and plastid markers for *L. laeve*).

Table 1. List of all species used in this study with species names, voucher specimens, and countries (RBGK = Royal Botanic Gardens, Kew)

Species	Collector	Number	Country
Calamus aruensis	Dransfield, J.D.	7571	Indonesia
Eremospatha barendii	Couvreur, T.L.P.	409	Cameroon
Eremospatha cabrae	Harris, D.J.	9547	Republic of Congo
Eremospatha cuspidata	Bruneau, A.	1071	Cameroon
Eremospatha dransfieldii	Ouattara & Stauffer	S-D 7	Ghana
Eremospatha haullevilleana	Harris, D.J.	9623	Republic of Congo
Eremospatha hookeri	Baker, W.J.	1364	Cultivated (RBGK)
Eremospatha laurentii	Valkenburg, J.L.C.H. van	2991	Gabon
Eremospatha macrocarpa	Couvreur, T.L.P.	399	Cameroon
Eremospatha wendlandiana	Couvreur, T.L.P.	382	Cameroon
Eugeissona tristis	Baker, W.J.	501	Malaysia
Laccosperma acutiflorum	Couvreur, T.L.P.	375	Cameroon
Laccosperma korupensis	Couvreur, T.L.P.	394	Cameroon
Laccosperma laeve	Valkenburg, J.L.C.H. van	2629	Gabon
Laccosperma opacum1	Couvreur, T.L.P.	403	Cameroon
Laccosperma opacum2	Ouattara, D.	15	Ghana
Laccosperma robustum1	Couvreur, T.L.P.	368	Cameroon
Laccosperma robustum2	Wieringa, J.J.	5166	Gabon
Laccosperma secundiflorum1	Couvreur, T.L.P.	369	Cameroon
Laccosperma secundiflorum2	Ouattara & Stauffer	S-D 12	Ghana
Lepidocaryum tenue	?	?	Peru
Mauritia flexuosa	Couvreur, T.L.P.	194	Bolivia
Mauritiella armata	Couvreur, T.L.P.	257	Bolivia
Metroxylon salomonense	Zona, S.	651	Solomon Islands
Oncocalamus macrospathus	Valkenburg, J.L.C.H. van	2628	Gabon
Oncocalamus mannii	Dransfield, J.D.	7007	Cameroon
Oncocalamus tuleyi	Sunderland, T.C.H.	1759	Cameroon
Raphia hookeri	Ouattara & Stauffer	3	Ghana
Raphia palma-pinus	Ouattara & Stauffer	14	Ghana

Table 2. List of the plastid and nuclear primers used for PCR amplifications in this study

Markers	Primers	5′ Sequence 3′	Annealing temperature
Plastid	psbA (F)	GTTATGCATGAACGTAATGCTC	60
	trnH (R)	CGCGCATGGTGGATTCACAAATC	
	psbZ (F)	GGTACMTACTTATTGAAT	58
	TrnfM (R)	GCGGAGTAGAGCAGTTTG	
	Rps3 (F)	TTCGGCTTTCGTCTCGGTAGG	60
	Rpl16 (R)	AACTCACACCATCCATTTCAA	
	atpI (F)	TAT TTA CAA GYG GTA TTC AAG CT	58
	atpH (R)	CCA AYC CAG CAG CAA TAA C	
Nuclear	WRKY 7 (F)	AAGGAACTCTGCTTCTTCTCA	55
	WRKY 7 (R)	GGATCATGTGATGCCCTCTCTA	
	PRK (F)	GTGATATGGAAGAACGTGG	55
	PRK (R)	ATTCCAGGGTATGAGCAGC	
	RPB2 (F)	CAACTTATTGAGTGCATCATGG	55
	RPB2 (R)	CCACGCATCTGATATCCAC	
	AGAMOUS 1 (F)	CAGGAATTTGATGGGAGAGTC	64
	AGAMOUS 1 (R)	GCTGATTGCTTTGCATGAG	
	Malate synthase (F)	TCTATCTCCCCAAGATGGAGCA	53–62
	Malate synthase (R)	CATTGGCTGCCGGATTAT	

NGS BIOINFORMATICS

Initial quality control, adapter removal and demultiplexing (mismatch of 0) of all reads generated by 454 Sequencing were undertaken directly by Eurofins MWG. We used the PRGmatic pipeline (Hird, Brumfield & Carstens, 2011) to undertake our analyses. PRGmatic generates a high quality pseudo reference genome based on the data, to which all reads are then aligned. In the first step, all high percentage identity reads for each individual are clustered together to form an allele. Pairs of alleles are then clustered under a lower identity percentage into contigs or loci. These loci are used to generate the pseudo reference genome to which all the reads are aligned.

We ran PRGmatic independently on all the reads for each barcoded individual after demultiplexing. The following parameters were set differently from default values: minimum number of reads to call high confidence alleles = 4; and minimum coverage for calling consensus sequence in an individual = 4. Once the individual genotypes were determined for each species we conducted additional checks to eliminate paralogues. First, for each identified locus per individual, we undertook a BLASTn search (Altschul *et al.*, 1990) against all sequences on GenBank. Loci that were identified as belonging to one of the target markers were kept, the others were removed from the dataset. Second, we separated targeted regions from unknown paralogues. Prior to this study, Sanger sequenced references for all markers (except WRKY7) and for one or two species of Ancistrophyllinae were available in GenBank. Thus, if several loci blasted to the same marker (e.g. PRK), we ran neighbour-joining analyses in Geneious to separate them using the GenBank sequence as a correct reference.

PHYLOGENETIC ANALYSES

For each individual nuclear marker dataset we undertook preliminary phylogenetic analyses using RAxML (see below) to identify potentially conflicting markers. Incongruence between markers was detected as different relationships with significant bootstrap support (>90%). Phylogenies were inferred using all data (plastid and nuclear; nine markers in total, see Table 2) under maximum parsimony (MP) and then maximum likelihood (ML). All MP analyses were performed using PAUP* (Swofford, 2002). One hundred replicates of random stepwise addition with subsequent tree-bisection-reconnection (TBR) branch swapping were carried out. A strict consensus tree was calculated from the resulting sample of the most parsimonious trees. MP bootstrap analysis (Felsenstein, 1985) was performed with 1000 replicates. For each bootstrapped dataset, a single random addition tree was constructed and swapped with TBR, keeping a maximum of five trees in memory. All ML analyses were carried out with RAxML v.7.2.6 (Stamatakis, 2006; Stamatakis, Hoover & Rougemont, 2008) accessed through the CIPRES Portal 2.1 (Miller *et al.*, 2009)(www.phylo.org). Phylogenetic tree inference using ML/rapid bootstrapping on XSEDE was used with default parameters (GTR + Γ model sequence evolution). One hundred bootstrap replicates were performed for ML phylogeny inference using the rapid bootstrap algorithm

(Stamatakis *et al.*, 2008) associated with a 'ML search' and 'estimate proportion of invariable sites'.

Bayesian analyses of phylogeny

Bayesian estimation of phylogeny was undertaken using BEAST v.1.8.1 under a relaxed molecular clock with uncorrelated lognormal distribution (Drummond & Rambaut, 2007). This also allowed us to estimate divergence times across lineages by integrating phylogenetic and fossil data. The combined matrix of plastid and nuclear markers was used with six independent partitions (one for each nuclear marker and the combined plastid DNA markers). Separate substitution models were inferred for all data partitions, as determined by jModelTest (Posada, 2008). One fossil calibration and one secondary calibration were used. For the fossil calibration we used the fossil of *Eremospatha chilgaensis* A.D.Pan, B.F.Jacobs, J.Dransf. & W.J.Baker from the late Oligocene period (27–28 Mya) (Pan *et al.*, 2005). This fossil represents a single thick leaflet with a single basally positioned robust spine and clearly distinct parallel venation. Pan *et al.* (2005) suggested that this leaflet strongly resembles leaves of *Eremospatha* 'by having heavily armed, thickened, reduced proximal leaflets with robust spines'. In contrast, other genera of Ancistrophyllinae (*Laccosperma* and *Oncocalamus*) are generally characterized by leaflets with non–thickened margins and slender spines (Sunderland, 2012). The authors suggested that this fossil closely resembles *E. dransfieldii* Sunderl. However, although we agree that this fossil belongs to *Eremospatha*, we prefer to assign it conservatively to the stem node of the genus. Our dating scheme thus represents minimum age estimations. The secondary calibration point was taken from the palm-wide dated chronogram inferred by Couvreur, Forest & Baker (2011a) to constrain the root node of our tree (crown node of Calamoideae) to 80 Mya. We used two different calibration schemes to estimate the potential impact of the fossil position on the divergence ages: (1) only the secondary calibration; and (2) the combined secondary and fossil calibrations. For the first scheme, the secondary calibration (root) was constrained by a normal prior ranging from 70–100 Mya corresponding broadly to the 95% confidence intervals inferred in Couvreur *et al.* (2011a). In the second scheme, the root was constrained by a normal prior as above, in addition to an exponential prior set for the fossil of *Eremospatha* with a mean of 0.5 and offset value of 27. A tree prior speciation birth–death model with incomplete sampling was used based on a ML inferred ultrametric starting tree using r8s (Sanderson, 2003). The analysis was run for 20 million generations and sampled every 1000th generation. Effective sample sizes (ESS values) for all parameters were examined in Tracer v1.6 (Rambaut & Drummond, 2003) to ensure that they were >200. To explore if our data and priors were both in agreement with one another, a 'sample from prior only' analysis was performed. TreeAnnotator was used to calculate posterior distributions of node ages and generate a maximum clad credibility (MCC) tree. Tree representation was performed in FigTree v.1.3.1 (http://tree.bio.ed.ac.uk/software/figtree/).

Hypothesis testing

We use phylogenetic simulations to test if trees simulated under different extinction hypotheses deviate significantly from the reconstructed phylogenetic trees (Crisp & Cook, 2009; Antonelli & Sanmartin, 2011). In all subsequent analyses, we used the results from calibration scheme 2 (see results). First, analyses were conducted on a sub-selection of 100 trees sampled equally every 2000 trees from our BEAST analyses and the MCC tree. Second, all outgroups and duplicated taxa (see below) were pruned. Third, to take missing taxon sampling into account, we calculated the sampling fraction of 0.81: 18 species sampled out of 22 species in total (including a potential cryptic species from West Africa, see Results). In addition, other undetected cryptic species could be a potential problem with our dataset, thus we repeated all analyses with a sampling fraction of 0.5 (reflecting that we sampled just 50% of the true diversity).

The average speciation (λ) and extinction (μ) rates, the extinction fraction (μ/λ) and the diversification rate ($\lambda - \mu$) across the selected 100 posterior trees using the function *birthdeath* implemented in the R package APE were estimated (Paradis, Claude & Strimmer, 2004).

Our hypotheses A and B (Fig. 1, Table 3 for parameters) were tested using simulations by comparing the shape of lineage-through-time (LTT) plots from simulated phylogenies to our observed LTT plot from reconstructed phylogenetic trees. We simulated phylogenies under a constant birth–death rate process using the R function *sim.rateshift.taxa* of the package TreeSim (Stadler, 2011). This function defines one or several punctual extinction events at a time (t) with a number of lineages surviving the extinction ('frac') and rates of speciation (λ) and extinction (μ) before (λ_1 and μ_1) and after this extinction event (λ_2 and μ_2). In all cases, two values of 'frac' were tested: 80% of lineages go extinct (frac = 0.2); and 95% of lineages go extinct (frac = 0.05). For λ_2 and μ_2 we used three values representing different hypotheses about how a clade could have reacted to a mass extinction event: 1.

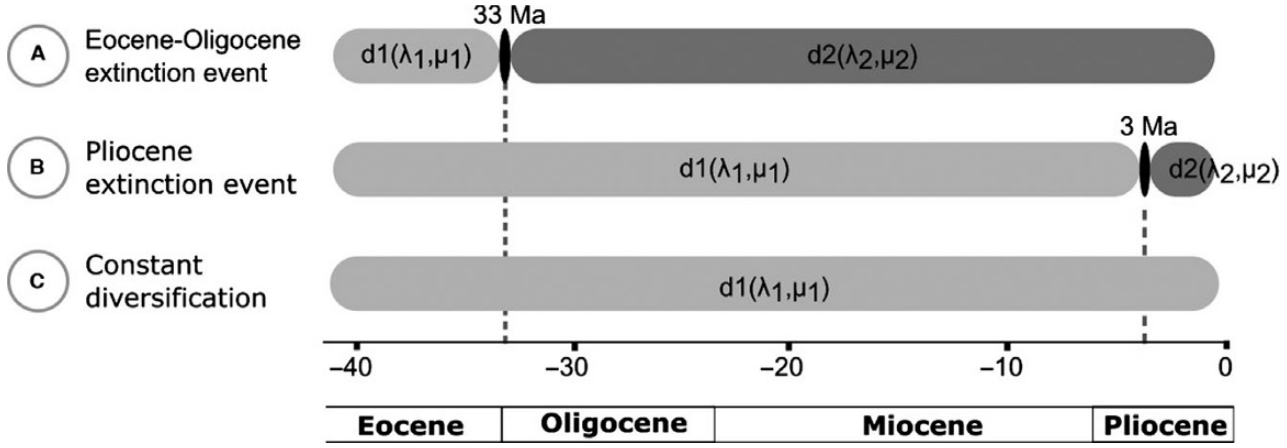

Figure 1. The three different evolutionary hypotheses tested in our study. Under hypotheses A and B, the rate of diversification changes from a diversification rate d1 (speciation rate: λ_1, extinction rate: μ_1) to d2 (λ_2, μ_2) after an extinction event (represented by a black bar) with the fraction of species that go extinct ranging from high (95% of all species go extinct) to moderate (80% of all species go extinct). Under hypothesis C a constant diversification rate is simulated with no rate shifts or mass extinctions. See Table 3 for parameters used.

Table 3. Diversification parameters used in this study. λ_1 and λ_2 refer to the speciation rate before and after the extinction event (EE), respectively, and μ_1 and μ_2 correspond to extinction rate before and after the extinction event, respectively

		Parameters before EE		Parameters after EE		
Hypotheses	Sub-hypotheses	λ_1	μ_1	λ_2	μ_2	Extinction fraction (%)
A (33 Mya)	a	0.1	0.03	0.1	0.03	95
	b	0.1	0.03	0.2	0.03	95
	c	0.1	0.03	0.1	0.06	95
	d	0.1	0.03	0.1	0.03	80
	e	0.1	0.03	0.2	0.03	80
	f	0.1	0.03	0.1	0.06	80
B (3 Mya)	a	0.1	0.03	0.1	0.03	95
	b	0.1	0.03	0.2	0.03	95
	c	0.1	0.03	0.1	0.08	95
	d	0.1	0.03	0.1	0.03	80
	e	0.1	0.03	0.2	0.03	80
	f	0.1	0.03	0.1	0.08	80
C (constant)	a	0.1	0.05			N/A

Speciation rates increased as more ecological opportunities became available: speciation rate changed from $\lambda_1 = 0.1$ to $\lambda_2 = 0.2$; extinction rate unchanged $\mu_2 = \mu_1 = 0.03$. 2. Extinction rates increased as the clade did not recover after the mass extinction: speciation rate remains unchanged at $\lambda_1 = \lambda_2 = 0.1$ and extinction rate increases from $\mu_1 = 0.03$ to $\mu_2 = 0.05$. 3. No change in rates of diversification occurred after the extinction episode ($\mu_2 = \mu_1 = 0.03$ and $\lambda_1 = \lambda_2 = 0.1$). The function also takes incomplete taxon sampling into account by defining a fraction of extant species sampled (here 0.86 or 0.5, see above).

For each of the hypotheses 1000 phylogenies were simulated. Parameters for each simulation are given in Table 3: (A) the 'ancient event' hypothesis with an extinction event at the Eocene–Oligocene boundary at 33 Mya; (B) the 'recent extinction event' hypothesis with an extinction event during the late Pliocene–early Pleistocene at 3 Mya; and (C) null hypothesis of constant diversification rates: we

simulated a constant diversification using the R function *sim.bd.taxa*.

The root age of all simulated phylogenies were constrained to the age of the root of our empirical phylogenetic tree by subtracting branching time values to the empirical phylogenetic tree root age. LTT plots were then generated for the empirical and the simulated phylogenetic trees. To compare the empirical reconstructed and simulated phylogenetic trees we used the APE R function *ltt.plot.coords* to extract the LTT plot coordinates by transforming each simulated phylogeny into a two-column matrix (column 1 = times and column 2 = number of lineages). The time and the number of lineages were then normalized. Using the 1000 matrices obtained after 1000 simulations we calculated the 95% confidence interval (CI) for each simulation. For each of the simulated phylogenies, we applied the same method as above by extracting time and number of lineage values before normalization.

To compare the empirical and simulated LTT plots we followed the methodology of Paradis (2015) in which the proportion of empirical points falling within the 95% confidence interval (CI) of the simulated LTT plots are counted and averaged. The higher the proportion of empirical points falling within the 95% CI of the simulated LTT plots, the higher the similarity between the empirical and simulated LTT plots. The 100 LTT plots derived from the 100 posterior trees sampled from BEAST were compared with the 95% CI of the 1000 simulated trees under each hypothesis. We thus report an average percentage of points (and the standard deviation) per empirical LTT plot found within the 95% CI of each of the simulated LTT plots.

RESULTS

Plastid dataset

Among the four plastid markers used, *atpI–atpH* was the most informative with 38 potentially informative sites (out of a total of 814 bp), and *rps3–rpl16* was the least informative with nine potentially informative sites (see Faye *et al.*, 2014). Alignment and concatenation of all plastid markers resulted in a dataset containing 28 sequences and 2888 characters of which 127 are variable. Among the variable characters 65 were potentially parsimony informative and 62 were uninformative.

454 Sequencing

Two hundred thousand reads were generated from ¼ of a 454 plate, of which 160 000 were correctly identified with a barcode (0 mismatches). Read length varied between 350–1000 bp with a mean of 635 bp and a median of 574 bp. Reads assigned to individual barcodes varied from 31 to 25 556, underlying a high heterogeneity in sequencing efficiency between barcodes. However, most barcodes had >100 reads. PRGmatic analyses were able to identify most of the markers. Paralogous sequences were found for most markers, even those suggested as being single or double copies. For AGAMOUS 1 and WRKY7, we detected several paralogous sequences and for PRK and RPB2 we detected fewer. Malate synthase was the least problematic of the markers with one or no identifiable paralogues. Sequences that clustered together with the respective reference sequence using neighbour joining were kept for further analyses. This hidden paralogous diversity led to significantly fewer reads per target marker than theoretically calculated before the run. Thus, in some cases, read coverage was low, generally 5–8×. For some species, some markers were not sequenced, because only the paralogues were sequenced or because they were not enough reads (>3× in coverage). GenBank numbers for all sequences are provided in Data S2.

Phylogenetics

No well supported conflicts were identified between the five nuclear markers and thus all nine markers including the plastid data were concatenated into a single dataset of 28 taxa comprising 6508 bp with alignment gaps retained. Parsimony analyses of the combined plastid and nuclear dataset yielded parsimonious trees with a consistency index (CI) of 0.85, a retention index (RI) of 0.84 and a re-scaled consistency index (RC) of 0.71. Results of MP and ML analyses were topologically compatible except relationships among *Laccosperma* spp. Monophyly of Ancistrophyllinae was confirmed with a strong bootstrap support (100%) in ML and MP analyses (Fig. 2). The clade was also resolved as monophyletic in the Bayesian analyses of the combined data with 1.0 posterior probability (PP). The genera *Eremospatha*, *Laccosperma* and *Oncocalamus* were also recovered as monophyletic with a strong support of bootstrap in all analyses. Relationships between the three genera were resolved with strong support values (Fig. 2). *Eremospatha* and *Laccosperma* were well supported as sister clades with 95% and 100% of bootstrap in MP and ML, respectively. In *Eremospatha*, *E. dransfieldii* and *E. cabrae* (De Wild. & T.Durand) DeWild. were recovered as sister species with strong support and together they were sister to the rest of the genus, showing a high genetic differentiation. Among the other *Eremospatha* spp., *E. hookeri* (G.Mann & H.Wendl.) H.Wendl. and *E. haullevilleana* De Wild. formed a moderately

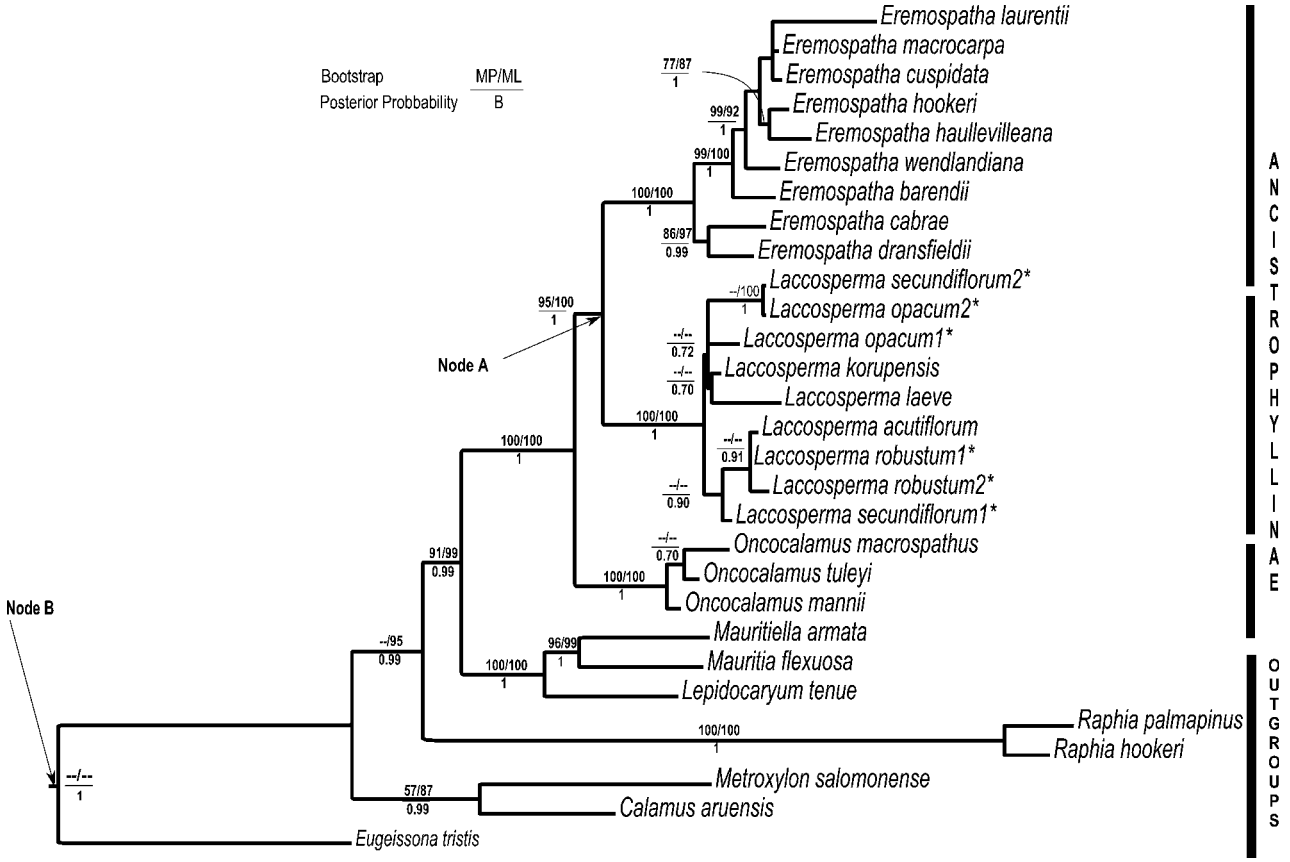

Figure 2. Maximum likelihood phylogram of subtribe Ancistrophyllinae and the eight outgroup species. Bootstrap values from the maximum parsimony (MP) and maximum likelihood (ML) analyses are indicated above branches (MP/ML). Posterior probabilities from the Bayesian analysis are under the branches. – = bootstrap values <87%; * = polyphyletic species. Node A represents the fossil calibration used under the molecular dating scheme 1. Node B corresponds to the secondary calibration point used in the molecular dating schemes 1 and 2 (crown node of Calamoideae).

supported group with 77% in MP, 87% in ML and 1.00 PP in the Bayesian analyses and were resolved as sister to the unsupported group *E. cuspidata* (G.Mann & H.Wendl.) H.Wendl., *E. macrocarpa* Schaedtler and *E. laurentii* De Wild. In *Laccosperma*, two groups of four species each were found in the ML analysis, but not in the MP analysis. In *Oncocalamus*, relationships between the three species remain less supported; *O. macrospathus* Burret and *O. tuleyi* Sunderl. form a sister pair, but this is not well supported (MP: 69%, ML: 58%).

Age estimation and diversification time

Both calibration schemes returned highly compatible results with slight age differences for some nodes (Table 4). All ESS for all parameters were >200, and the 'sample from prior only' analysis showed that priors had little effect on our data. Even in the first scheme when only using a secondary calibration, the stem node age of *Eremospatha* was estimated to be 25 Mya [95% highest posterior distribution (HPD): 14.3–38.2], nearly identical to the age assigned using the fossil calibration (27 Mya). Under the two calibration schemes, Ancistrophyllinae originated during the Eocene with a stem node inferred at 46.8 Mya (95% HPD: 36–58) for calibration 1 and 44 Mya in calibration 2 (95% HPD: 27–61 Mya) (Fig. 3). The crown node age was estimated to the late Eocene–early Oligocene 32 Mya (95% HPD: 27–37) for calibration 1 and 30 Mya (95% HPD: 17–44 Mya) for calibration 2. Diversification analyses of the phylogenetic tree inferred a moderate level of extinction rate and a low diversification rate within the Ancistrophyllinae (Table 5).

LTT plots comparison

Using calibration scheme 2, the empirical LTT plot of the reconstructed phylogeny based on the MCC

Table 4. Ages and 95% confidence intervals of the highest posterior distribution (HPD) of selected clades as inferred from relaxed-clock Bayesian dating analyses. Bold values indicate calibration values. Calibration 1 = Root + stem *Eremospatha*, Calibration 2 = Root. ESS, Effective Sample Size

	Calibration 1			Calibration 2		
Node	Age (Mya)	HPD 95%	ESS	Age (Mya)	HPD 95%	ESS
1. Root Height	**79.6365**	**[71.83, 86.99]**	**7537**	**79.4303**	**[71.42, 87.21]**	18001
2. *Eremospatha* crown	16.612	[11.30, 22.02]	725	15.612	[8.07, 23.78]	540
3. *Eremospatha* stem	**27.4757**	**[27, 28.43]**	14768	25.6543	[14.39, 38.20]	595
4. *Laccosperma* crown	9.7228	[5.18, 14.78]	575	8.9088	[4.00, 14.28]	525
5. *Oncocalamus* crown	8.0076	[2.76, 14.51]	1740	7.5292	[2.22, 14.44]	1212
6. Ancistrophyllinae crown	32.3312	[27.98, 37.90]	1987	30.3243	[17.16, 44.08]	627
7. Ancistrophyllinae stem	46.8062	[36.17, 58.25]	744	44.8626	[27.24, 61.36]	707
8. Mauritiinae stem	67.06	[52.13, 81.01]	916	64.8431	[44.40, 83.04]	670

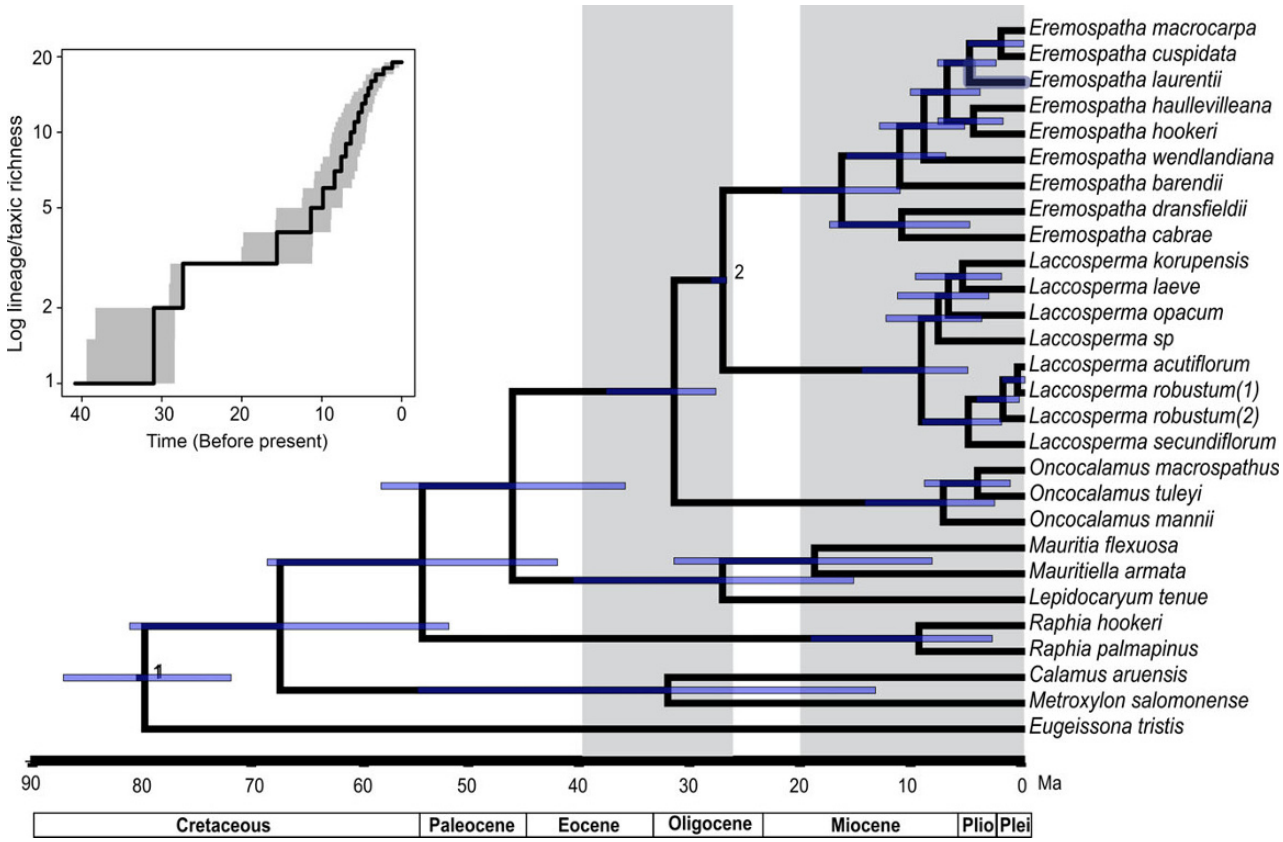

Figure 3. Chronogram of subtribe Ancistrophyllinae from the BEAST analysis under calibration scheme 2. 1: position of the fossil of *Eremospatha chilgaensis*, 2: position of the secondary calibration (crown node of Calamoideae). The scale axis shows ages in millions of years. Bars around nodes indicate 95% density intervals of the posterior distribution of node ages.

tree and the mean LTT plot resulting from 100 trees sampled from the posterior distribution showed an anti-sigmoidal curve (Fig. 3). The LTT plots indicate an early increase in diversification from the stem node of Ancistrophyllinae at 46 Mya until 33 Mya. This was followed by a plateau of low or no diversification, which was subsequently replaced by a new phase of increased diversification starting at *c.* 15 Mya.

Simulations using two different sampling fractions (0.86 and 0.50), resulted in highly similar results (Table 6). Simulations for hypothesis A provided an average of empirical points between 84.3% and 92.5% falling inside the 95% CI plot suggesting a

strong resemblance between both LTT plots (Fig. 4A). For hypothesis B, between 20.1% and 22.6% of the empirical points fell inside the 95% simulated CI (Fig. 4B). When compared with a null model computed with a constant birth death scenario (hypothesis C), 72.9% of empirical points fell inside the 95% simulated CI.

DISCUSSION

Phylogeny and evolution of African rattans

The phylogenetic relationships between the three genera of Ancistrophyllinae remained weakly resolved or unresolved in past morphological and molecular studies (Baker *et al.*, 2000a,b, 2009; Asmussen *et al.*, 2006; Faye *et al.*, 2014). Our analyses that includes five nuclear and four plastid markers show for the first time that *Eremospatha* is strongly supported as sister to *Laccosperma*, and together they are strongly supported as sister to *Oncocalamus* (Fig. 2). The relationship found here was weakly supported in both the supermatrix (70% bootstrap value) and supertree (s = 6, where s is the number of input trees supporting a given node) phylogenetic trees of Baker *et al.* (2009). The phylogenetic tree of Baker & Dransfield (2000a) also indicated some moderate support for the sister relationship between *Eremospatha* and *Laccosperma* (86% bootstrap values based on the ribosomal

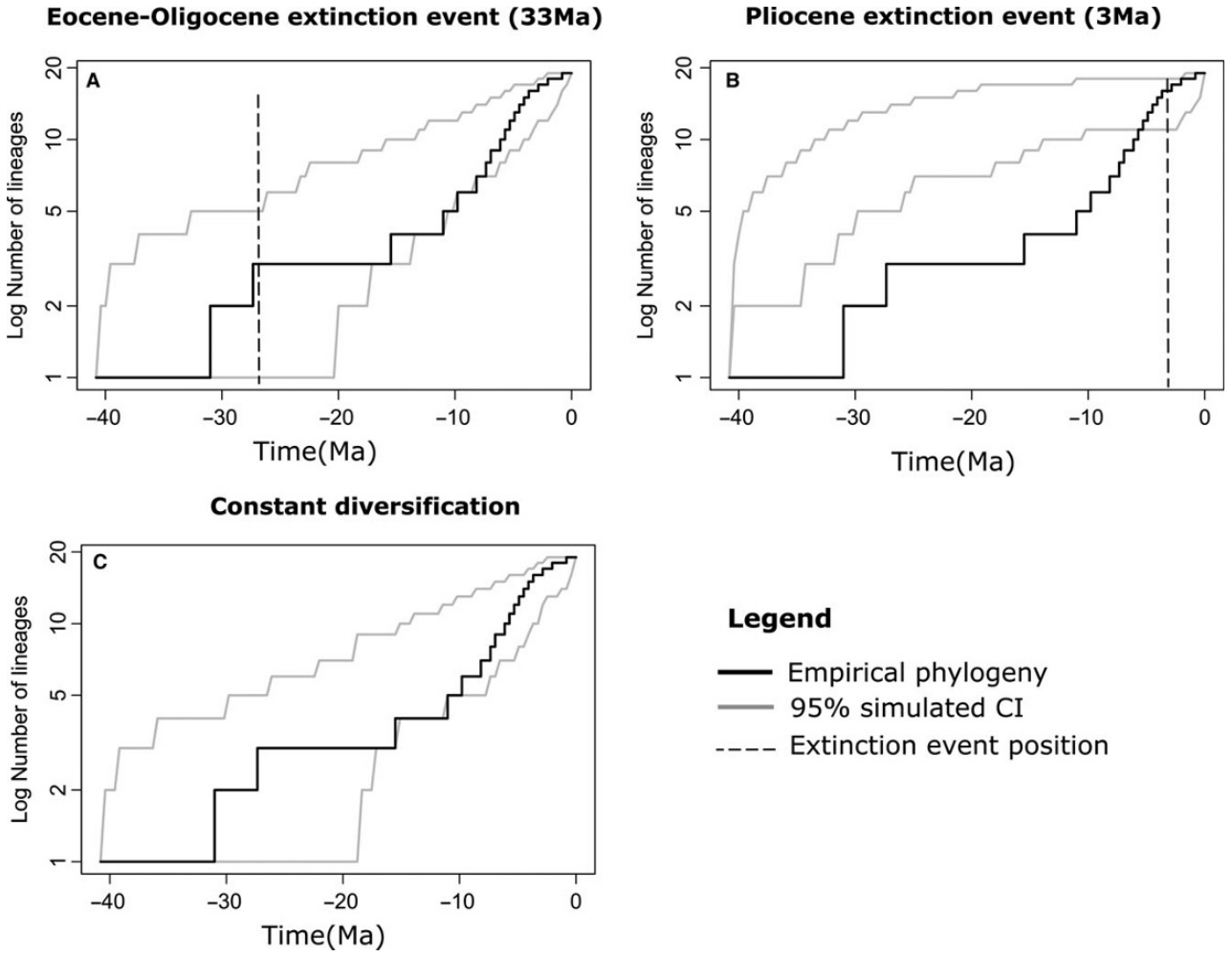

Figure 4. Overlay of empirical and simulated phylogenetic trees under different hypotheses of extinction in Africa. Figures represent the overlay of the mean LTT plot from the 100 trees sampled from our BEAST analyses (solid black line) with the 95% simulated confidence interval of 1000 simulated phylogenies (solid grey lines). Speciation (λ) and extinction rates (μ) were estimated using the R function *bd*. A, An extinction event at 33 Mya with constant speciation and extinction rate before and after the extinction event ($\lambda_1 = \lambda_2 = 0.1$, $\mu_1 = \mu_2 = 0.03$) and an extinction fraction of 95%. B, the same as in A but with a mass extinction at 3 Mya. C: Constant diversification rate.

internal transcribed spacer (ITS) region and the plastid *rps16* intron). At the morphological level this relationship is supported by, for example, floral characters (Sunderland, 2012). Both these genera are characterized by hermaphroditic flowers grouped in pairs (dyads), whereas *Oncocalamus* has unisexual monoecious flowers grouped in a complex cluster. For other characters, however, this relationship is not supported, for example, life history traits: *Laccosperma* is hapaxanthic (individual stems die after a single flowering event), whereas, *Eremospatha* and *Oncocalamus* are pleonanthic (continuous flowering) (Sunderland, 2012). Our results further strongly support the sister relationship between Ancistrophyllinae and Mauritiinae (*Mauritia* L.f.–*Mauritiella* Burret–*Lepidocaryum* Mart.), with Raphiinae (*Raphia* P.Beauv.) sister to this group. The phylogenetic relationships between these three subtribes remains ambiguous based on morphology (Baker *et al.*, 2000a), plastid and/or nuclear markers (Baker *et al.*, 2000a,b; Asmussen *et al.*, 2006) or supertree/supermatrix approaches (Baker *et al.*, 2009). Our results should, however, be taken with caution, as the sampling of other genera of Calamoideae remains limited and this aspect was not the purpose of this study.

Faye *et al.* (2014) suggested that this difficulty in achieving strong support values between genera of Ancistrophyllinae might be the result of an early rapid diversification. Our results somewhat support this hypothesis as all three genera are estimated to have originated during the Oligocene between 31.7 Mya and 27.0 Mya. Each genus is then subtended by a long branch or 'temporal gap' before the diversification of its extant species after 15 Mya (Fig. 3). Early diversification is suggested to generate morphological diversity (Foote, 1997), which tends to increase over time (Harmon *et al.*, 2003). In addition the greater age of clades is expected to be positively correlated with morphological change (Purvis, 2004; Ricklefs, 2006). Thus, the important morphological diversity found between genera of Ancistrophyllinae could be explained by their origins in the Oligocene followed by a long period of independent evolution.

In *Eremospatha*, the sister relationship between *E. cabrae* and *E. dransfieldii* suggested by Faye *et al.* (2014) is confirmed. These species are morphologically different and show an allopatric distribution, with *E. cabrae* distributed across Central Africa and *E. dranfieldii* in West Africa (Sunderland, 2012). These species diverged during the mid and late Miocene 11.6 Mya (95% HPD 5–17.6 Mya), just after the Middle Miocene Climatic Transition (14 Mya). This event led to renewed cooling and aridity across Africa breaking up the once continuous rain forest (Couvreur *et al.*, 2008). Shifts in habitats are known to cause species divergence (Losos, Warheit & Schoener, 1997; Reznick *et al.*, 1997) and play a prominent role in speciation (Smith *et al.*, 1997; Schluter, 1998). This ecological divergence can lead to a burst of diversification with the acquisition of reproductive isolation ('ecological speciation') (Rundell & Price, 2009). Thus the speciation of these *Eremospatha* spp. could be the result of a climate-driven vicariance event due to the breakup of the rain forest during the middle Miocene.

Impact of past extinction events on diversification in Ancistrophyllinae

The overall lower species diversity of African rain forests when compared with the Neotropics and South East Asia has intrigued scientists for decades (Richards, 1996; Couvreur, 2015). Here, we tested two main hypotheses about extinction on the evolutionary dynamics of African rattans. Our results suggest that this clade has undergone moderate levels of extinction (extinction fraction = 0.272; Table 5) since its origin in the late Palaeocene/early Eocene. Extinction in palms is particularly evident when analysing the palm fossil record where extinction and turnover in morphospecies are often documented across Africa and at different time periods (Salard-Cheboldaeff, 1990; Morley, 2000; Pan *et al.*, 2005; Jacobs, Pan & Scotese, 2010). In addition, the important morphological disparity between the three genera of Ancistrophyllinae was also suggested as the result of important extinction linked to climate change in Africa (Dransfield, 1988; Baker & Dransfield, 2000). The empirical LTT plot (Fig. 3, insert) shows an antisigmoidal pattern that could possibly be associated with the signature of a mass extinction event (Crisp & Cook, 2009). The 'plateau' of the LTT plot occurs between 30 Mya and 25 Mya, just after the Eocene–

Table 5. Diversification parameters inferred from the crown node of Ancistrophyllinae. The λ and μ parameters represent speciation and extinction rates respectively. These were estimated from the 100 posteriors phylogenetic trees. The extinction fraction rate is the ratio λ/μ representing the fraction of species going extinct and the diversification rate corresponds to the difference between λ and μ

Root node	λ	μ	Extinction fraction	Diversification rate
Mean	0.103	0.032	0.272	0.071
Standard deviation	0.019	0.029	0.233	0.014

Oligocene boundary, which has been suggested to have severely impacted palm species diversity (Hypothesis A) (Pan *et al.*, 2005). All three rattan genera had evolved at that time, but then underwent a 'temporal gap' (high extinction or low speciation) which might explain the large morphological disparity observed between them (Dransfield, 1988; Baker & Dransfield, 2000). In addition, the simulated LTT plots under the hypothesis of a mass extinction event at 33 Mya (hypothesis A) agrees well with our empirical LTT. Indeed, an average between 88.1 and 92.5% of all points fell inside the 95% CI of the simulated phylogenies depending on the scenario simulated (Fig. 4, Table 6Aa–Af) providing additional support for this hypothesis. The Oligocene–Eocene boundary saw a relatively sudden drop in global temperatures (Zachos *et al.*, 2001). This drop is thought to have led to important reduction in plant species diversity in the Neotropics (Jaramillo, Rueda & Mora, 2006). Molecular phylogenetic analyses have also detected signatures of this mass extinction event at *c.* 30 Mya, e.g. in two independently evolving lineages in African and Australian tribes of Fabaceae (Crisp & Cook, 2009). The congruent ages of these possible extinction events between independent lineages and African rattans suggest a common response to a global event. This global event appears to have negatively impacted plant diversity in general and tropical rain forests diversity in particular on every continent (Morley, 2000; Couvreur, 2015). Thus, the Eocene–Oligocene boundary would only in part explain why African rain forests have lower species diversity as most regions would have been negatively impact by this event.

Table 6. Fit of the simulated lineage through time (LTT) plots under different extinction hypotheses to the empirical (reconstructed) LTT plot, following the method of Paradis (2015). For each hypothesis, 1000 simulations were run under the three different hypotheses (see Table 3 for parameter values) with a sampling fraction of 0.86 (14% of species not sampled) and 0.5 (50% of species not sampled). The table indicates the mean empirical (ME) points and its associated standard deviation (SD) falling inside the 95% confidence interval (CI) of the empirical LTT

	Sampling fraction 0.86		Sampling fraction 0.5	
Hypotheses	ME	SD	ME	SD
A (33 Mya)				
a	92.5	5.4	97.4	4.4
b	92.5	5.4	93.5	5.3
c	88.1	7.2	90.1	6.2
d	91.0	5.1	91.0	3.1
e	84.3	7.6	85.3	8.6
f	92.1	6.0	95.1	5.2
B (3 Mya)				
a	21.3	5.4	27.3	4.5
b	20.1	4.6	25.1	5.6
c	20.6	5.7	23.6	5.8
d	22.6	6.3	26.6	4.3
e	21.4	5.3	22.4	5.6
f	20.5	4.9	21.5	5.3
C (constant)				
a	72.9	6.3	72.9	6.3

In contrast, the hypothesis of an extinction event in palms during the Pliocene at 3 Mya is not supported by our data. This relatively recent period of increased aridity was suggested to be important in explaining lower species diversity across tropical Africa in plants in general (Morley, 2000; Plana, 2004) and palms in particular (Moore, 1973). In fact, our results suggest that African rattans mostly diversified during the late Miocene after 10 Mya (Fig. 3). This finding is in agreement with several other studies showing that plant species in Africa mainly originated during the Miocene and Pliocene, before the Pleistocene (e.g. Auvrey *et al.*, 2010; Couvreur *et al.*, 2011b; Yessoufou *et al.*, 2014). Our results highlight once more the important role of the late Miocene and Pliocene in the diversification of the African flora (Couvreur *et al.*, 2008) even in ancient lineages such as Ancistrophyllinae.

The constant diversification rate hypothesis (C) is not completely rejected by our data, with an average of 72.9% of points falling inside the 95% CI of the simulated LTT plots. Thus our data suggest that African rattans possibly diversified under a constant diversification rate, punctuated by a severe extinction event during the Eocene-Oligocene transition. This process can lead to LTT plots that resemble constant diversification (Crisp & Cook, 2009). A similar result was found in the African cycad genus *Encephalartos* Lehm., although on a much shorter time frame, that was suggested to diversify at a constant rate punctuated by a mass extinction event (Yessoufou *et al.*, 2014). Baker & Couvreur (2013a, b) found no evidence in their palm genus-level diversification analyses for a decrease in diversification rates in African lineages, including Ancistrophyllinae, suggesting that lower African palm species diversity might be the result of lower speciation rates when compared with other regions (Baker & Couvreur, 2013b). This situation contrasts with other studies of palm diversification in South America (e.g. *Astrocaryum* G.Mey., Roncal *et al.*, 2013) or South East Asia (e.g. Livistoninae, Bacon *et al.*, 2013) which have documented non-constant rates with significant increases in diversification rates at

the species level linked to dispersal or tectonic movements.

Our study has a number of limitations, however. First, the total number of species included in the study remains few (<20) and thus the power of our tests and simulations might be insufficient (Rabosky, 2010; Beaulieu & O'Meara, 2015). However, in the context of understanding clades of fewer/lower species diversity in Africa, this will be an inherent problem. Phylogenetic support at the species level could be improved, especially in *Laccosperma* and *Oncocalamus*, as it remains relatively weak even after sequencing nine markers (nuclear and plastid). Next generation sequencing of hundreds of nuclear loci within genera developed across palms (Heyduk *et al.*, 2016) could provide increased support and better dating of this clade. Third, if extinction did indeed play a major role in explaining present day diversity of the African flora, using phylogenetic trees of extant species only might be limiting. However, our results seem to fit well with what we know from the fossil record of palms, in that this family has been affected by extinction during the Oligocene–Eocene (Hypotheses A). More detailed, continent-wide analyses of the palm fossil record in Africa (e.g. Pan *et al.*, 2005) should provide future insights into the evolution of the African flora complementary to those of robust dated molecular phylogenetic trees.

ACKNOWLEDGEMENTS

We thank Emmanuel Paradis for sharing R scripts and unpublished results and Remi Tournebize and Angela Cano for help with R scripts. Terry Sunderland is thanked for help with the identification of herbarium material collected in the field. We are grateful to Fred Stauffer for sending silica gel dried material of West African species. We thank Fred Stauffer, Henrik Balslev and three other anonymous reviewers for their comments of a previous version of the manuscript. Funding from this project was provided by the International Foundation for Science (IFS) under grant number No. AI1D/30248, the International Palm Society (IPS) and International Association for Plant Taxonomy (IAPT) to the first author. The study was additionally funded by a grant 'Appuie aux Equipes des Recherches' of the Agence Universitaire de la Francophonie (AUF) 2013–2015 to Bonaventure Sonké. The IRD program 'Programme Pilote Régional: Changements globaux, biodiversité et santé dans les forêts tropicales humides d'Afrique centrale' is thanked for support towards Adama Faye's field work. Finally, we dedicate this work to our friend and colleague, Dr Jean-Christophe Pintaud, who passed away suddenly in August 2015. He was an inspiring figure in palm research and is greatly missed.

REFERENCES

Al-Qurainy F, Khan S, Al-Hemaid FM, Ali MA, Tarroum M, Ashraf M. 2011. Assessing molecular signature for some potential date (*Phoenix dactylifera* L.) cultivars from Saudi Arabia, based on chloroplast DNA sequences *rpoB* and *psbA-trnH*. *International Journal of Molecular Sciences* **12:** 6871–6880.

Altschul SF, Gish W, Miller W, Myers EW, Lipman DJ. 1990. Basic local alignment search tool. *Journal of Molecular Biology* **215:** 403–410.

Antonelli A, Sanmartin I. 2011. Mass extinction, gradual cooling, or rapid radiation? Reconstructing the spatiotemporal evolution of the ancient angiosperm genus *Hedyosmum* (Chloranthaceae) using empirical and simulated approaches. *Systematic Biology* **60:** 596–615.

Asmussen CB, Dransfield J, Deickmann V, Barfod AS, Pintaud JC, Baker WJ. 2006. A new subfamily classification of the palm family (Arecaceae): evidence from plastid DNA phylogeny. *Botanical Journal of the Linnean Society* **151:** 15–38.

Auvrey G, Harris DJ, Richardson JE, Newman MF, Sarkinen TE. 2010. Phylogeny and dating of *Afromomum* (Zingiberarceae). In: Seberg O, Peterson G, Barfod AS, Davis JI, eds. *Diversity, phylogeny, and evolution in the monocotyledons*. Århus: Aarhus University Press, 287–305.

Axelrod DI, Raven PH. 1978. Late Cretaceous and Tertiary vegetation history of Africa. In: Werger MJA, ed. *Biogeography and ecology of southern Africa*. The Hague: W. Junk bv Publishers, 77–130.

Bacon CD, Michonneau F, Henderson AJ, McKenna MJ, Milroy AM, Simmons MP. 2013. Geographic and taxonomic disparities in species diversity: dispersal and diversification rates across Wallace's line. *Evolution* **67:** 2058–2071.

Baker WJ, Couvreur TLP. 2013a. Global biogeography and diversification of palms sheds light on the evolution of tropical lineages. Historical biogeography. *Journal of Biogeography* **40:** 274–285.

Baker WJ, Couvreur TLP. 2013b. Global biogeography and diversification of palms sheds light on the evolution of tropical lineages. II: diversification history and origin of regional assemblages. *Journal of Biogeography* **40:** 286–289.

Baker WJ, Dransfield J. 2000. Towards a biogeographic explanation of the calamoid palms. In: Wilson KL, Morrison DA, eds. *Monocots: systematics and evolution*. Melbourne: CSIRO, 545–553.

Baker WJ, Dransfield J, Hedderson TA. 2000a. Phylogeny, character evolution, and a new classification of the calamoid palms. *Systematic Botany* **25:** 297–322.

Baker WJ, Hedderson TA, Dransfield J. 2000b. Molecular phylogenetics of subfamily Calamoideae (Palmae) based on

nrDNA ITS and cpDNA *rps16* intron sequence data. *Molecular Phylogenetics and Evolution* **14:** 195–217.

Baker WJ, Savolainen V, Asmussen-Lange C, Chase M, Dransfield J, Forest F, Harley M, Uhl N, Wilkinson M. 2009. Complete generic-level phylogenetic analyses of palms (Arecaceae) with comparisons of supertree and supermatrix approaches. *Systematic Biology* **58:** 240–256.

Beaulieu JM, O'Meara BC. 2015. Extinction can be estimated from moderately sized molecular phylogenies. *Evolution* **69:** 1036–1043.

Blach-Overgaard A, Balslev H, Dransfield J, Normand S, Svenning J-C. 2015. Global-change vulnerability of a key plant resource, the African palms. *Scientific Reports* **5:** 1–10.

Blach-Overgaard A, Kissling WD, Dransfield J, Balslev H, Svenning J-C. 2013. Multimillion year climatic effects on palm species diversity in Africa. *Ecology* **94:** 2426–2435.

Blach-Overgaard A, Svenning JC, Dransfield J, Greve M, Balslev H. 2010. Determinants of palm species distributions across Africa: the relative roles of climate, non-climatic environmental factors, and spatial constraints. *Ecography* **33:** 380–391.

Bybee SM, Bracken-Grissom H, Haynes BD, Hermansen RA, Byers RL, Clement MJ, Udall JA, Wilcox ER, Crandall KA. 2011. Targeted amplicon sequencing (TAS): a scalable next-gen approach to multi-locus, multi-taxa phylogenetics. *Genome Biology and Evolution* **3:** 1312–1323.

Couvreur TLP. 2015. Odd man out: why are there fewer plant species in African rain forests? *Plant Systematics and Evolution* **301:** 1299–1313.

Couvreur TLP, Baker WJ. 2013. Tropical rain forest evolution: palms as a model group. *BMC Biology* **11:** 48.

Couvreur TLP, Chatrou LW, Sosef MSM, Richardson JE. 2008. Molecular phylogenetics reveal multiple tertiary vicariance origins of the African rain forest trees. *BMC Biology* **6:** 54.

Couvreur TLP, Forest F, Baker WJ. 2011a. Origin and global diversification patterns of tropical rain forests: inferences from a complete genus-level phylogeny of palms. *BMC Biology* **9:** 44.

Couvreur TLP, Porter-Morgan H, Wieringa JJ, Chatrou LW. 2011b. Little ecological divergence associated with speciation in two African rain forest tree genera. *BMC Evolutionary Biology* **11:** 296.

Crisp MD, Cook LG. 2009. Explosive radiation or cryptic mass extinction? Interpretating signatures in molecular phylogenies. *Evolution* **63:** 2257–2265.

Dransfield J. 1988. The palms of Africa and their relationships. In: Goldblatt P, Lowry PP, eds. *Modern systematic studies in African botany*. St Louis: Missouri Botanical Garden Press, 95–103.

Dransfield J, Uhl NW, Asmussen CB, Baker WJ, Harley MM, Lewis CE. 2008. *Genera Palmarum: the evolution and classification of palms*. Kew: Kew Publishing.

Drummond AJ, Rambaut A. 2007. BEAST: Bayesian evolutionary analysis by sampling trees. *BMC Evolutionary Biology* **7:** 214.

Faye A, Pintaud JC, Baker WJ, Sonké B, Couvreur TLP. 2014. A plastid phylogeny of the African rattans (Ancistrophyllinae, Arecaceae). *Systematic Botany* **39:** 1099–1107.

Felsenstein J. 1985. Confidence limits on phylogenetics: an approach using the bootstrap. *Evolution* **39:** 783–791.

Foote M. 1997. The evolution of morphological diversity. *Annual Review of Ecology and Systematics* **28:** 129–152.

Gentry AH. 1993. Diversity and floristic composition of lowland tropical forest in Africa and South America. In: Goldblatt P, ed. *Biological relationships between Africa and South America*. New Haven: Yale University Press, 500–547.

Harmon LJ, Schulte JA, Larson A, Losos JB. 2003. Tempo and mode of evolutionary radiation in iguanian lizards. *Science* **301:** 961–964.

Heyduk K, Trapnell DW, Barrett CF, Leebens-Mack J. 2016. Phylogenomic analyses of species relationships in the genus *Sabal* (Arecaceae) using targeted sequence capture. *Biological Journal of the Linnean Society* **117:** 106–120.

Hird SM, Brumfield RT, Carstens BC. 2011. PRGmatic: an efficient pipeline for collating genome-enriched second-generation sequencing data using a 'provisional-reference genome'. *Molecular Ecology Resources* **11:** 743–748.

Jacobs BF, Kingston JD, Jacobs LL. 1999. The origin of grass-dominated ecosystems. *Annals of the Missouri Botanical Garden* **86:** 590–643.

Jacobs BF, Pan AD, Scotese CR. 2010. A review of the Cenozoic vegetation history of Africa. In: Werdelin L, Sanders WJ, eds. *Cenozoic mammals of Africa*. Berkeley: University of California Press, 57–72.

Jaramillo C, Rueda MJ, Mora G. 2006. Cenozoic plant diversity in the Neotropics. *Science* **311:** 1893–1896.

Kenfack D, Thomas DW, Chuyong G, Condit R. 2007. Rarity and abundance in a diverse African forest. *Biodiversity and Conservation* **16:** 2045–2074.

Kissling WD, Baker WJ, Balslev H, Barfod A, Borchsenius F, Dransfield J, Govaerts R, Svenning J. 2012a. Quaternary and pre Quaternary historical legacies in the global distribution of a major tropical plant lineage. *Global Ecology and Biogeography* **21:** 909–921.

Kissling WD, Eiserhardt WL, Baker WJ, Borchsenius F, Couvreur TLP, Balslev H, Svenning J-C. 2012b. Cenozoic imprints on the phylogenetic structure of palm species assemblages worldwide. *Proceedings of the National Academy of Sciences* **109:** 7379–7384.

Lewis CE, Doyle JJ. 2001. Phylogenetic utility of the nuclear gene malate synthase in the palm family (Arecaceae). *Molecular Phylogenetics and Evolution* **19:** 409–420.

Lewis CE, Doyle JJ. 2002. A phylogenetic analysis of tribe Areceae (Arecaceae) using two low-copy nuclear genes. *Plant Systematics and Evolution* **236:** 1–17.

Linder HP. 2001. Plant diversity and endemism in sub-Saharan tropical Africa. *Journal of Biogeography* **28:** 169–182.

Linder HP. 2014. The evolution of African plant diversity. *Frontier in Genetics* **2:** 38.

Losos JB, Warheit KI, Schoener TW. 1997. Adaptive differentiation following experimental island colonization in *Anolis* lizards. *Nature* **387:** 70–73.

Ludeña B, Chabrillange N, Aberlenc-Bertossi F, Adam H, Tregear JW, Pintaud J-C. 2011. Phylogenetic utility of the nuclear genes AGAMOUS 1 and PHYTOCHROME B in palms (Arecaceae): an example within Bactridinae. *Annals of Botany* **108:** 1433–1444.

Mauro-Herrera M, Meerow AW, Borrone JW, Kuhn DN, Schnell RJ. 2006. Ten informative markers developed from WRKY sequences in coconut (*Cocos nucifera*). *Molecular Ecology Notes* **6:** 904–906.

Meerow AW, Noblick L, Borrone JW, Couvreur TLP, Mauro-Herrera M, Hahn WJ, Kuhn DN, Nakamura K, Oleas NH, Schnell RJ. 2009. Phylogenetic analysis of seven WRKY genes across the palm subtribe Attaleinae (Arecaceae) identifies *Syagrus* as sister group of the coconut. *PLoS ONE* **4:** e7353.

Miller MA, Holder MT, Vos R, Midford PE, Liebowitz T, Chan L, Hoover P, Warnow T. 2009. *The CIPRES portals*. CIPRES. http://www.phylo.org/sub_sections/portal.

Moore HEJ. 1973. Palms in the tropical forest ecosystems of Africa and South America. In: Meggers BJ, Ayensu ES, Duckworth WD, eds. *Tropical forest ecosystems of Africa and South America: a comparative review*. Washington: Smithsonian Institution Press, 63–88.

Morley RJ. 2000. *Origin and evolution of tropical rain forests*. New York: John Wiley & Sons.

Morlon H. 2014. Phylogenetic approaches for studying diversification. *Ecology Letters* **17:** 508–525.

Pan AD, Jacobs BF, Dransfield J, Baker WJ. 2005. The fossil history of palms (Arecaceae) in Africa and new records from the Late Oligocene (28–27 Mya) of north–western Ethiopia. *Botanical Journal of the Linnean Society* **151:** 69–81.

Paradis E. 2015. Random phylogenies and the distribution of branching times. *Journal of Theoretical Biology* **387:** 39–45.

Paradis E, Claude J, Strimmer K. 2004. APE: analyses of phylogenetics and evolution in R language. *Bioinformatics* **20:** 289–290.

Plana V. 2004. Mechanisms and tempo of evolution in the African Guineo-Congolian rainforest. *Philosophical Transactions of the Royal Society B-Biological Sciences* **359:** 1585–1594.

Posada D. 2008. jModelTest: phylogenetic model averaging. *Molecular Biology and Evolution* **25:** 1253–1256.

Purvis A. 2004. Evolution: how do characters evolve? *Nature* **432:** 338–341.

Rabosky DL. 2010. Extinction rates should not be estimated from molecular phylogenies. *Evolution* **64:** 1816–1824.

Rakotoarinivo M, Dransfield J, Bachman SP, Moat J, Baker WJ. 2014. Comprehensive Red List assessment reveals exceptionally high extinction risk to Madagascar palms. *PLoS ONE* **9:** e103684.

Rambaut A, Drummond AJ. 2003. *Tracer. version 1.4*. Available from http://evolve.zoo.ox.ac.uk/

Reznick DN, Shaw FH, Rodd FH, Shaw RG. 1997. Evaluation of the rate of evolution in natural populations of guppies (*Poecilia reticulata*). *Science* **275:** 1934–1937.

Richards PW. 1973. Africa, the 'odd man out'. In: Meggers BJ, Ayensu ES, Duckworth WD, eds. *Tropical forest ecosystems of Africa and South America: a comparative review*. Washington: Smithsonian Institution Press.

Richards PW. 1996. *The tropical rain forest: an ecological study*, 2nd edn. Cambridge: Cambridge University Press.

Ricklefs RE. 2005. Historical and ecological dimensions of global patterns in plant diversity. *Biologiske Skrifter* **55:** 583–603.

Ricklefs RE. 2006. Time, species, and the generation of trait variance in clades. *Systematic Biology* **55:** 151–159.

Roncal J, Francisco-Ortega J, Asmussen CB, Lewis CE, Hoot SB. 2005. Molecular phylogenetics of tribe Geonomeae (Arecaceae) using nuclear DNA sequences of phosphoribulokinase and RNA polymerase II. *Systematic Botany* **30:** 275–283.

Roncal J, Kahn F, Millan B, Couvreur TLP, Pintaud J-C. 2013. Cenozoic colonization and diversification patterns of tropical American palms: evidence from *Astrocaryum* (Arecaceae). *Botanical Journal of the Linnean Society* **171:** 120–139.

Rundell RJ, Price TD. 2009. Adaptive radiation, nonadaptive radiation, ecological speciation and nonecological speciation. *Trends in Ecology & Evolution* **24:** 394–399.

Salard-Cheboldaeff M. 1990. Intertropical African palynostratigraphy from Cretaceous to late Quaternary times. *Review of Palaeobotany and Palynology.* **28:** 365–368.

Sanderson MJ. 2003. r8s: inferring absolute rates of molecular evolution and divergence times in the absence of a molecular clock. *Bioinformatics* **19:** 301–302.

Scarcelli N, Barnaud A, Eiserhardt W, Treier UA, Seveno M, d'Anfray A, Vigouroux Y, Pintaud J–C. 2011. A set of 100 chloroplast DNA primer pairs to study population genetics and phylogeny in monocotyledons. *PLoS ONE* **6:**e19954.

Schluter D. 1998. Ecological causes of speciation. In: Howard DJE, Berlcocher SH, eds. *Endless forms: species and speciation*. New York: Oxford University Press, 3–15.

Sepulchre P, Ramstein G, Fluteau F, Schuster M, Tiercelin JJ, Brunet M. 2006. Tectonic uplift and Eastern Africa aridification. *Science* **313:** 1419–1423.

Smith TB, Wayne RK, Girman DJ, Bruford MW. 1997. A role for ecotones in generating rainforest biodiversity. *Science* **276:** 1855–1857.

Stadler T. 2011. Simulating trees with a fixed number of extant species. *Systematic Biology* **60:** 676–684.

Stamatakis A. 2006. RAxML–VI–HPC: maximum likelihood–based phylogenetic analyses with thousands of taxa and mixed models. *Bioinformatics* **22:** 2688–2690.

Stamatakis A, Hoover P, Rougemont J. 2008. A rapid bootstrap algorithm for the RAxML web–servers. *Systematic Biology* **57:** 758–771.

Stauffer F, Ouattara D, Stork AL. 2014. Palmae. In: J–P Lebrun, AL Stork, eds. *Tropical African flowering plants. Monocotyledons 2*. Geneva: Conservatoire et Jardin botaniques de la Ville de Genève, Switzerland, 326–354.

Sunderland TCH. 2012. A taxonomic revision of the rattans of Africa (Arecaceae: Calamoideae). *Phytotaxa* **51:** 1–76.

Swofford DL. 2002. *PAUP* phylogenetic analysis using parsimony (* and other methods), v. 4.0 beta 10*. Sunderland: Sinauer Associates.

Terborgh J, Davenport LC, Niangadouma R, Dimoto E, Mouandza JC, Schultz O, Jaen MR. 2016. The African rainforest: odd man out or megafaunal landscape? African and Amazonian forests compared. *Ecography* **39:** 187–193.

Yessoufou K, Bamigboye SO, Daru BH, van der Bank M. 2014. Evidence of constant diversification punctuated by a mass extinction in the African cycads. *Ecology and Evolution* **4:** 50–58.

Zachos J, Pagani M, Sloan L, Thomas E, Billups K. 2001. Trends, rhythms, and aberrations in global climate 65 Mya to present. *Science* **292:** 686–693.

SUPPORTING INFORMATION

Additional Supporting Information may be found in the online version of this article:

Data S1. Trageted Amplicon Sequencing (TAS) method.

Data S2. Genbank numbers.